An Adaptive Control System for Variable Mass Quad-Rotor UAV Involved in Rescue Missions

Xiao LIANG*, Guodong CHEN, Jiahui WANG, Zheyuan BI, Peng SUN

School of Automation, Shenyang Aerospace University, Shenyang, Liaoning, 110136, China

***Abstract* — Because the mass of quad-rotor helicopter Unmanned Aerial Vehicles (UAV) changes after delivering relief supplies, an adaptive control strategy based on model reference adaptation is proposed. First a quad-rotor model is established based on the Quanser 3-DOF hover platform. Then a control strategy is developed consisting of two layers: a baseline controller using a Linear Quadratic Regulator (LQR) and Model Reference Adaptive Controller (MRAC) to eliminate the impact of load change. In simulation, the results illustrate that the strategy can improve the effectiveness of the control system when the mass and the moment of inertia change in applications such as rescue missions.**

Keywords - quad-rotor; rescue mission; variable mass; linear quadratic regulator; model reference adaptive control

I. INTRODUCTION

In May 12th 2008, a deadly earthquake of Richter 8.0 hit Sichuan Province of China. Though the rescue teams repaired the roads immediately, the ground vehicles still could not reach the core of the disaster in time. The characteristics of low-cost and three-dimensional movement make quad rotor is more suitable in rescue mission [1]. In April 20th 2013, another earthquake of Richter 7.0 occurred in Sichuan Province again. The National Geological Disaster Emergency Technical Center (NGDETC) sent several portable quad rotors, and finished the geological survey at 1000 meters during 20 minutes. However, the quad rotors just can perform the inspection at high altitudes currently, but not deliver the relief supplies.

Quad rotor is portable and can take off vertically, so the researches have attracted a lot of attention around the world. Quad rotor is a multi-variable, non-linear, highly coupled, and under actuated system. The researches about control law most focus on PID, robust control, sliding mode control and intelligent control.

TABLE 1. TYPICAL CONTROL METHODS OF GENERAL QUAD ROTOR

Method	Characteristics	Application
PID	The system is divided into several separate channels, and control laws are designed respectively. The method is classic and easy to implement [2].	Attitude [3] Height [4] Hover [5] Trajectory [6]
Back-stepping	The virtual control is designed by state equation. Control laws are calculated by Lyapunove function. The adjustment time is short, and it is suitable for on-line control.	Attitude [7] Position [8] Hover [9] Tracking [10]
Sliding mode control	According to certain logic, make the state slid on the sliding face and reach equilibrium finally by changing feedback control structure. It is insensitive to the model error, parameter uncertainty and other interferences [11].	Attitude, Position [12]
Quaternion control	The attitude is described in quaternion method which is simple and no singular point. Control law is designed based on state feedback or output feedback [13].	Attitude [14]
Neural network	Neural network is used to figure out the inverse of nonlinear model. The nonlinear mapping ability can find the relationship between the intermediate variable and the actual input.	Attitude [15]

Before and after delivering, the mass of quad rotor will change. But the modeling and control of variable mass aircraft mainly focus on fire control problem, such as the sudden change of mass caused by the delivery of laser-guided missiles and bombs [16]. Other variable mass control involves heavy equipment airdrop [17] and aerial refueling [18]. And the hot issue focuses on the modeling and control of slowly changing center of gravity.

The change of mass caused by the delivery of weapon is relatively small compared to the whole aircraft. But the relief supplies account for a substantial part of quad rotor, and

DOI 10.5013/ IJSSST.a.17.29.22 ISSN: 1473-804x online, 1473-8031 print

Quad rotor is far less than conventional aircraft. Furthermore, compared to aerial refueling, the delivery of relief supplies is a momentary change process. Therefore, the control of variable mass quad rotor in rescue mission has its own specialty, and it requires targeted research.

Quad rotor is a helicopter unmanned aerial vehicles which has light weight and small power, so it is sensitive to the changes of mass, and the change of parameters is likely to cause significantly reduce of system performance. Focusing on the problem of variable mass quad rotor before and after delivering relief supplies, this paper establish a dynamics model of quad rotor based on QstudioRP hardware-in-the-loop simulation platform firstly. Then a linear quadratic baseline controller is designed for flight attitude, and which constitute a reference model. Next, a model reference adaptive controller is used to reduce the impact of mass. The simulation results show that by using the proposed method, the system performance approaches the situation before delivering relief supplies.

II. HARDWARE-IN-THE-LOOP SIMULATION PLATFORM OF QUADROTOR

QStudioRP simulation platform is developed by Quanser in Canada. It is an integrated open platform for control system development, design, simulation and test [19]. The platform can make system modeling (using Maple software), real-time simulation (using Wincon software), rapid control prototyping (RCP), hardware-in-the-loop (HIL) test and simulation. Because the platform has the advantages of low cost, low risk, fast development, high availability and maintainability, it gradually raises the attention of many researchers.

A. *Hardware System of Simulation Platform*

The hardware system mainly includes motor/rotor, encoder (sensor), power modules and quad rotor, which are shown in Fig. 1 and listed in Table 2.

Figure 1. Main structure of hardware system

TABLE 2. DEVICE SPECIFICATIONS

Name	Value
Helicopter body mass	$1.39kg$
Helicopter body length	$48cm$
Base dimensions	$17.5cm \times 17.5cm$
Encoder resolution	$8192\, counts/rev$
Pitch angle range	$75(\pm 37.5\deg)$
Yaw angle range	$360\deg$
Propeller diameter	$20.3cm$
Propeller pitch	$15.2cm$
Motor armature resistance	0.83Ω
Motor current-torque constant	$0.0182\, N \cdot m/A$

Main components of the platform are as follows:

(1) Q8 hardware-in-loop control card: it is universal, and can make high-performance real-time measurement. It has 8 channels of A/D (14bit), 8 channels of D/A (12bit), 8 channels of incremental encoders, and 2 channels of PWM. Digital I/O is 32bit, and can sample all encoders and analog ports simultaneously.

(2) Motor: The platform uses brushless DC motor. The resistance is 0.83 ohm, and current torque constant is 0.0182 N m/A. Its rated voltage is 12V, peak voltage is 22V, and maximum speed is 5600 rpm. The platform is equipped by four motors. Front and back motor influence the pitch channel, left and right motor influence the roll channel, and four motors influence the yaw channel.

(3) Power Modules: The product is UPM-2405. Four motors use power modules.

(4) Encoder: Three encoders are used to detect the attitude angle of three-axis (pitch angle, roll angle, yaw angle). The encoders counts 8192 per revolution, and the resolution of three-axis is up to 0.0439°.

(5) Rotor and Frame: The length of rotor is 20/15 cm, and thrust-moment coefficient is 0.119N/V. The frame has plastic base, and four clips which ensure the equilibrium of initial state. The collecting rings are installed on the base, and they allow the quad rotor rotate around the base.

B. *Software System of Simulation Platform*

Software uses real-time digital process control software Wincon, which has high performance on RCP and HIL. It is able to run Simulink model of Matlab, and it is convenient to adjust parameters.

It is easy to use Wincon to construct a real-time system. Wincon has been seamlessly integrated to the products of MathWorks, so the programs of Matlab can be verified in the actual hardware platform. Specially, the core of RTX ensures the processes have a higher CPU priority.

The mathematical model and controller in this paper are all developed by Matlab. Then the programs of Matlab are converted to C language by Wincon. After compiling, the codes drive hardware platform to achieve desired command.

III. SYSTEM DESCRIPTION

Assumption [20]:

(1) The structure is supposed to be rigid and strictly symmetrical.

(2) The center of mass and the body fixed frame origin are assumed to coincide.

(3) The moment is proportional to the DC motor voltage.

(4) The change of attitude angle range is limited into $(-5^{\circ},5^{\circ})$.

(5) The air resistance can be ignored at low speed.

The quadrotor is motivated by four motors and can lead to three attitudes, i.e. yaw, pith, roll. The front and rear rotors rotate in a clockwise direction while the left and right rotors rotate in a counter-clockwise direction to balance the torque created by the spinning rotors.

Define $v=(x,y,z,\psi,\theta,\phi)\in R^6$, let $\xi=(x,y,z)\in R^3$ presents the position, $\eta=(\psi,\theta,\phi)\in R^3$ respectively denote yaw, pitch and roll angle. Then we can get that the kinetic energy of motion $T_{trans}=1/2m\xi^T\xi$ and the kinetic energy of rotation $T_{rot}=1/2m\eta^T\eta$, where m represents the mass of airframe. Ignoring the line movement and using the Lagrange method, the dynamic model of the four-rotor helicopter can be presented as Equation (1) [21].

$$\begin{cases}\ddot{\psi}=\dfrac{K_{tc}}{J_y}l(V_f+V_b)+\dfrac{K_{tn}}{J_y}l(V_r+V_l)\\ \ddot{\theta}=\dfrac{K_f}{J_p}l(V_r-V_l)\\ \ddot{\phi}=\dfrac{K_f}{J_r}l(V_f-V_b)\end{cases}\tag{1}$$

where K_{tc}, K_{tn} are respectively counter rotation propeller torque-thrust constant and normal rotation propeller torque-thrust constant. J_y is equivalent moment of inertia about the yaw axis, J_p is equivalent moment of inertia about the pitch axis, J_r is equivalent moment of inertia about the roll axis. K_f is the propeller force-thrust constant which is found by experiment. V_f, V_b, V_r and V_l respectively represent the front, back, right and left motor voltage of the system.

IV. DESIGN OF THE CONTROLLER FOR VARIABLE MASS QUADROTOR

Control strategy focuses on the attitude channel. Firstly, design the baseline controller based on Linear Quadratic Regulator (LQR). Secondly, baseline and simplified model constitute the reference model. Thirdly, design the adaptive controller to reduce the influence brought by delivering relief supplies.

A. Baseline Controller Based on Linear Quadratic Regulator (LQR)

Define the state vector $x(t)=[\psi,\theta,\phi,\dot{\psi},\dot{\theta},\dot{\phi}]\in R^n$, output vector $y(t)=[\psi,\theta,\phi]\in R^q$, input vector $u(t)=[V_f,V_b,V_r,V_l]^T$. After linearization, the state equation of attitude channel is:

$$\begin{cases}\dot{\boldsymbol{x}}_a(t)=\boldsymbol{A}_a\boldsymbol{x}_a(t)+\boldsymbol{B}_a\boldsymbol{u}_a(t)\\ \boldsymbol{y}_a(t)=\boldsymbol{C}_a\boldsymbol{x}_a(t)\end{cases}\tag{2}$$

According to the theory of Linear Quadratic Regulator (LQR), the controller is:

$$\boldsymbol{u}_a(t)=-\boldsymbol{L}_a\boldsymbol{x}_a(t)+\boldsymbol{L}_{ra}\boldsymbol{h}_a(t)\tag{3}$$

where $\boldsymbol{L}_a$ and $\boldsymbol{L}_{ra}$ is feedback gain matrix and feedforward gain matrix, respectively. $\boldsymbol{h}_a$ is input command. Choose the performance indicator is:

$$\begin{aligned}J=&\frac{1}{2}\boldsymbol{e}_a^{\ T}(t_f)\boldsymbol{S}\boldsymbol{e}_a(t_f)\\&+\frac{1}{2}\int_{t_0}^{t_f}[\boldsymbol{e}_a^{\ T}(t)\boldsymbol{V}(t)\boldsymbol{e}_a(t)+\boldsymbol{u}_a^{\ T}(t)\boldsymbol{R}(t)\boldsymbol{u}_a(t)]dt\end{aligned}\tag{4}$$

In Equation (4), $\boldsymbol{e}_a=\boldsymbol{h}_a-\boldsymbol{y}_a$. $\boldsymbol{S}$, $\boldsymbol{V}(t)$, $\boldsymbol{R}(t)$ is respectively the weighting matrix of $\boldsymbol{e}_a(t_f)$, $\boldsymbol{e}_a(t)$, $\boldsymbol{u}_a(t)$. When performance indicator J reaches its minimum, there is:

$$\begin{cases}\boldsymbol{L}_a=\boldsymbol{R}^{-1}\boldsymbol{B}_a^{\ T}\overline{\boldsymbol{P}}\\ \boldsymbol{L}_{ra}=\boldsymbol{R}^{-1}\boldsymbol{B}_a^{\ T}[\overline{\boldsymbol{P}}\boldsymbol{B}_a\boldsymbol{R}^{-1}\boldsymbol{B}_a^{\ T}-\boldsymbol{A}_a^{\ T}]^{-1}\boldsymbol{C}_a^{\ T}\boldsymbol{V}\end{cases}\tag{5}$$

where $\overline{\boldsymbol{P}}$ is the solution of Riccati equation, and $\boldsymbol{V}$ and $\boldsymbol{R}$ is diagonal matrix. According to Equation (2) and (5), the closed-loop control system based on LQR is:

$$\begin{cases}\dot{\boldsymbol{x}}_a=(\overline{\boldsymbol{A}}_a-\overline{\boldsymbol{B}}_a\overline{\boldsymbol{L}}_a)\boldsymbol{x}_a+\overline{\boldsymbol{B}}_a\overline{\boldsymbol{L}}_{ra}\boldsymbol{h}_a\\ \boldsymbol{y}_a=\overline{\boldsymbol{C}}_a\boldsymbol{x}_a\end{cases}\tag{6}$$

When quadrotor has not delivered relief supplies, $\boldsymbol{A}_a$, $\boldsymbol{B}_a$ and $\boldsymbol{C}_a$ nearly do not change. So their value is respectively constant $\bar{\boldsymbol{A}}_a$, $\bar{\boldsymbol{B}}_a$ and $\bar{\boldsymbol{C}}_a$ in that case. From Equation (5), we know that $\boldsymbol{L}_a$ and $\boldsymbol{L}_{ra}$ is also constant $\bar{\boldsymbol{L}}_a$ and $\bar{\boldsymbol{L}}_{ra}$, respectively. Thus we use $\bar{\boldsymbol{L}}_a$ and $\bar{\boldsymbol{L}}_{ra}$ instead of $\boldsymbol{L}_a$ and $\boldsymbol{L}_{ra}$ in Equation (6). After delivering relief supplies, $\boldsymbol{A}_a$ and $\boldsymbol{B}_a$ deviate the original value of $\bar{\boldsymbol{A}}_a$ and $\bar{\boldsymbol{B}}_a$, and $\boldsymbol{L}_a$ and $\boldsymbol{L}_{ra}$ will deviate $\bar{\boldsymbol{L}}_a$ and $\bar{\boldsymbol{L}}_{ra}$ at the same time, respectively. The control performance based on LQR declines greatly, and even quad rotor will lose control. Therefore, model reference adaptive control (MRAC) is added to reduce the impact brought by the change of mass.

B. Controller Based on Model Reference Adaptation Control (MRAC)

The feedforward and feedback control law of MRAC associate LQR controller, and they constitute the controller together, which is shown in Fig. 2.

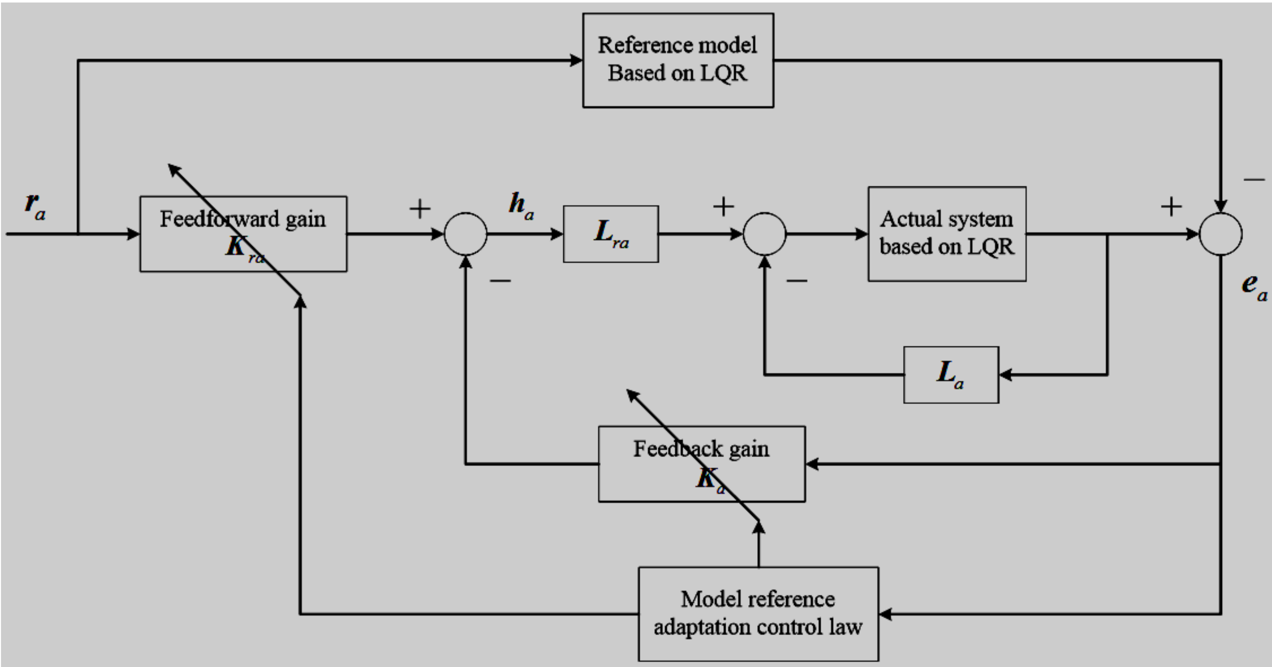

Figure 2. Adaptive control structure of attitude for variable mass quad rotor.

To the system in Fig. 2, according to Equation (6), the reference model is chosen as:

$$\begin{cases} \dot{\boldsymbol{x}}_{new} = \boldsymbol{A}_{new}\boldsymbol{x}_{new} + \boldsymbol{B}_{new}\boldsymbol{r}_a \\ \boldsymbol{y}_a = \boldsymbol{C}_{new}\boldsymbol{x}_{new} \end{cases} \tag{7}$$

where $\boldsymbol{A}_{new} = \bar{\boldsymbol{A}}_a - \bar{\boldsymbol{B}}_a\bar{\boldsymbol{L}}_a$, $\boldsymbol{B}_{new} = \bar{\boldsymbol{B}}_a\bar{\boldsymbol{L}}_{ra}$ and $\boldsymbol{C}_{new} = \bar{\boldsymbol{C}}_a$. After delivering relief supplies, parameters of quadrotor are changed, and the actual system will be:

$$\begin{cases} \dot{\boldsymbol{x}}_a = (\boldsymbol{A}_a - \boldsymbol{B}_a\bar{\boldsymbol{L}}_a)\boldsymbol{x}_a + \boldsymbol{B}_a\bar{\boldsymbol{L}}_{ra}\boldsymbol{h}_a \\ \boldsymbol{y}_a = \boldsymbol{C}_a\boldsymbol{x}_a \end{cases} \tag{8}$$

According to Equation (8), the controller is designed as:

$$\boldsymbol{h}_a = -\boldsymbol{K}_a\boldsymbol{x}_a + \boldsymbol{K}_{ra}\boldsymbol{r}_a \tag{9}$$

Here $\boldsymbol{r}_a$ is the desired input. $\boldsymbol{K}_{ra}$ and $\boldsymbol{K}_a$ is feedforward gain matrix and feedback gain matrix respectively. Suppose we have $\tilde{\boldsymbol{K}}_{ra}$ and $\tilde{\boldsymbol{K}}_a$ which make the closed-loop system is same to the reference model, then set $\Delta\boldsymbol{K}_{ra} = \boldsymbol{K}_{ra} - \tilde{\boldsymbol{K}}_{ra}$ and $\Delta\boldsymbol{K}_a = \boldsymbol{K}_a - \tilde{\boldsymbol{K}}_a$. Define error vector $\boldsymbol{e}_a = \boldsymbol{x}_{new} - \boldsymbol{x}_a$, so

$$\dot{\boldsymbol{e}}_a = \boldsymbol{A}_{new}\boldsymbol{e}_a + \boldsymbol{B}_{new}\tilde{\boldsymbol{K}}_{ra}^{-1}(\Delta\boldsymbol{K}_a\boldsymbol{x}_a - \Delta\boldsymbol{K}_{ra}\boldsymbol{r}_a) \tag{10}$$

Design Lyapnove function as:

$$L = \boldsymbol{e}_a{}^T\boldsymbol{P}_{new}\boldsymbol{e}_a + \boldsymbol{tr}(\Delta\boldsymbol{K}_a{}^T\Gamma\Delta\boldsymbol{K}_a + \Delta\boldsymbol{K}_{ra}{}^T\Gamma\Delta\boldsymbol{K}_{ra}) \tag{11}$$

DOI 10.5013/ IJSSST.a.17.29.22

ISSN: 1473-804x online, 1473-8031 print

where Γ is positive definite matrix. Because Equation (7) comes from the closed-loop system based on LQR which has not deliver relief supplies, the system is stable. So there is a matrix $\boldsymbol{P}_{new}$ and it satisfies $\boldsymbol{A}_{new}{}^T\boldsymbol{P}_{new}+\boldsymbol{P}_{new}\boldsymbol{A}_{new}=-\boldsymbol{Q}_a$, where $\boldsymbol{Q}_a$ is positive definite matrix. In addition, $\tilde{\boldsymbol{K}}_a$ and $\tilde{\boldsymbol{K}}_{ra}$ change slowly compared to $\boldsymbol{K}_a$ and $\boldsymbol{K}_{ra}$ respectively, so they can be taken as constants.

$$\begin{aligned}\dot{L}=&\boldsymbol{e}_a{}^T(\boldsymbol{A}_{new}{}^T\boldsymbol{P}_{new}+\boldsymbol{P}_{new}\boldsymbol{A}_{new})\boldsymbol{e}_a\\&+2\boldsymbol{e}_a{}^T\boldsymbol{P}_{new}\boldsymbol{B}_{new}\tilde{\boldsymbol{K}}_{ra}^{-1}(\Delta\boldsymbol{K}_a\boldsymbol{x}_a-\Delta\tilde{\boldsymbol{K}}_{ra}\boldsymbol{r}_a)\\&+2\boldsymbol{tr}(\Delta\boldsymbol{K}_a{}^T\Gamma\Delta\dot{\boldsymbol{K}}_a+\Delta\boldsymbol{K}_{ra}{}^T\Gamma\Delta\dot{\boldsymbol{K}}_{ra})\end{aligned}\tag{12}$$

According to the property of matrix trace, select:

$$\begin{cases}\Delta\dot{\boldsymbol{K}}_a=\dot{\boldsymbol{K}}_a=-\boldsymbol{B}_{new}{}^T\boldsymbol{P}_{new}\boldsymbol{e}_a\boldsymbol{x}_a{}^T\operatorname{sgn}(l)\\\Delta\dot{\boldsymbol{K}}_{ra}=\dot{\boldsymbol{K}}_{ra}=\boldsymbol{B}_{new}{}^T\boldsymbol{P}_{new}\boldsymbol{e}_a\boldsymbol{x}_a{}^T\operatorname{sgn}(l)\end{cases}\tag{13}$$

where $\operatorname{sgn}(l)$ is determined by $\tilde{\boldsymbol{K}}_{ra}$ whether it is positive or negative definite matrix. From Equation (12) and (13), there is:

$$\begin{aligned}\dot{L}&=\boldsymbol{e}_a{}^T(\boldsymbol{A}_{new}{}^T\boldsymbol{P}_{new}+\boldsymbol{P}_{new}\boldsymbol{A}_{new})\boldsymbol{e}_a\\&=\boldsymbol{e}_a{}^T(-\boldsymbol{Q}_a)\boldsymbol{e}_a<0\end{aligned}\tag{14}$$

Therefore, the model reference adaptive control law of the closed-loop system based on LQR is:

$$\begin{cases}\boldsymbol{K}_a=\int_0^t-\boldsymbol{B}_{new}{}^T\boldsymbol{P}_{new}\boldsymbol{e}_a\boldsymbol{x}_a{}^T\operatorname{sgn}(l)d\tau+\boldsymbol{K}_{a0}\\\boldsymbol{K}_{ra}=\int_0^t\boldsymbol{B}_{new}{}^T\boldsymbol{P}_{new}\boldsymbol{e}_a\boldsymbol{r}_a{}^T\operatorname{sgn}(l)d\tau+\boldsymbol{K}_{ra0}\end{cases}\tag{15}$$

Here, the solution of $\boldsymbol{A}_{new}{}^T\boldsymbol{P}_{new}+\boldsymbol{P}_{new}\boldsymbol{A}_{new}=-\boldsymbol{Q}_a$ is $\boldsymbol{P}_{new}$. $\boldsymbol{Q}_a$ is a unit matrix, and $\boldsymbol{r}_a$ is desired input. According to Equation (15) and the stability theory of Lyapnov, the general error of Equation (10) is global asymptotically stable, and the control performance will approach the situation of reference model in Equation (7).

V. SIMULATION VERIFICATION

In the simulation, the proposed method is tested in the system which is described in section 2. The parameters of the Quanser 3-DOF hovering system are displayed in Table 3.

TABLE 3. VALUES OF MODEL PARAMETERS

Symbol	Description	Value	Unit
K_{tn}	Normal rotation propeller torque-thrust constant	0.0036	$N\cdot m/V$
K_{tc}	Counter rotation propeller torque-thrust constant	-0.0036	$N\cdot m/V$
K_f	Propeller force-thrust constant found experimentally	0.1188	N/V
l	Distance between pivot and each motor	0.197	m
J_y	Equivalent moment of inertia about the yaw axis	0.110	$Kg\cdot m^2$
J_p	Equivalent moment of inertia about the pitch axis	0.0552	$Kg\cdot m^2$
J_r	Equivalent moment of inertia about the roll axis	0.0552	$Kg\cdot m^2$

According to the parameters in Table 3, the system matrices of Equation (2) are $\boldsymbol{A}_a=\begin{bmatrix}0&0&0&1&0&0\\0&0&0&0&1&0\\0&0&0&0&0&1\\0&0&0&0&0&0\\0&0&0&0&0&0\\0&0&0&0&0&0\end{bmatrix}$,

$$\boldsymbol{B}_a=\begin{bmatrix}0&0&0&0\\0&0&0&0\\0&0&0&0\\\frac{K_{tc}}{J_y}&\frac{K_{tc}}{J_y}&\frac{K_{tn}}{J_y}&\frac{K_{tn}}{J_y}\\\frac{lK_f}{J_p}&-\frac{lK_f}{J_p}&0&0\\0&0&\frac{lK_f}{J_r}&-\frac{lK_f}{J_r}\end{bmatrix}\text{ and }\boldsymbol{C}_a=\begin{bmatrix}1&0&0&0&0&0\\0&1&0&0&0&0\\0&0&1&0&0&0\end{bmatrix}.$$

At the beginning of simulation, quad rotor is given a step input. Fig. 3 and 4 are the control performance of pitch angle before and after delivering relief supplies, respectively. Solid line represents the PID control method, dotted line represents LQR method, and point line represents the MRAC method.

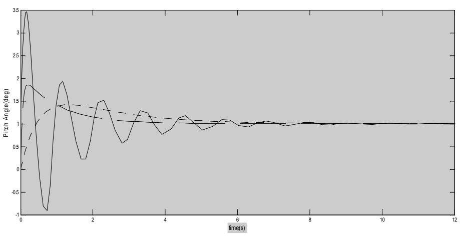

Figure 3. Performance of pitch angle with different controllers before delivering relief supplies

DOI 10.5013/ IJSSST.a.17.29.22 ISSN: 1473-804x online, 1473-8031 print

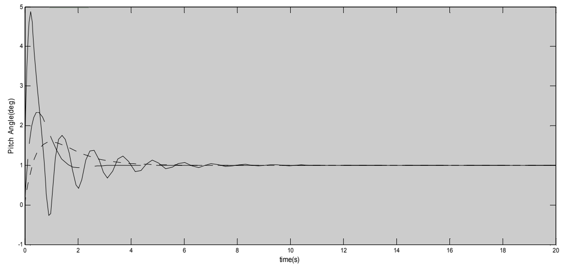

Figure 4. Performance of pitch angle with different controllers after delivering relief supplies

In Fig. 3, quad rotor has not delivered relief supplies yet. The controller based on LQR performances well, and it is better than PID method. In Fig. 4, quad rotor just delivered the supplies. Here, the mass of quad rotor reduces 30% in the simulation. Fig. 4 illustrates that the overshoots of three methods all increase, but the degree is different. The overshoot of PID is biggest, and MRAC is smallest. Compared Fig. 3 and Fig. 4, PID will spend more time to reach steady state after delivering relief supplies. The control of LQR also has concussion, and MRAC is the best.

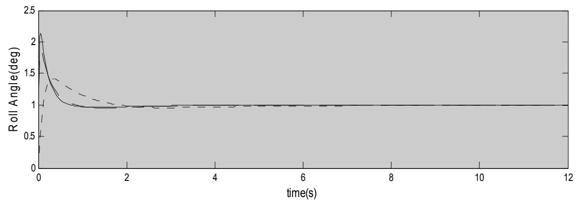

Figure 5. Performance of roll angle with different controllers before delivering relief supplies

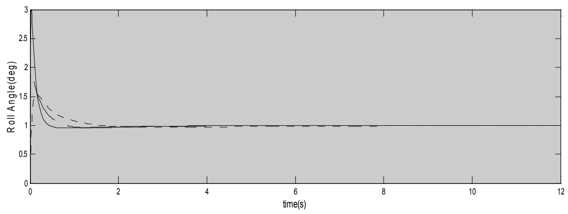

Figure 6. Performance of roll angle with different controllers after delivering relief supplies

Fig. 5 and 6 are the control performance of roll angle before and after delivering relief supplies, respectively. The mass of quad rotor also reduces 30% and quad rotor also has a step input at the beginning of simulation. Solid line represents the PID control method, dotted line represents LQR method, and point line represents the MRAC method.

In Fig. 5, quad rotor has not delivered relief supplies yet. And in Fig. 6, quad rotor just delivered the supplies. Compared with pitch angle, the influence on roll angle is smaller in general. From Fig. 5 and 6, the three methods expend a similar time to enter steady state, but the overshoots all increase after delivering relief supplies. The overshoot of PID changes from 2.1 to 3, and it changes from 1.4 to 1.6 in MRAC method. In LQR method, the overshoot maintains around 1.8. MRAC is also the best.

When the mass changes, the output of baseline controller deviates that of MRAC, so adaptive control law adjusts the parameters automatically. The simulations show that the method is able to ensure the control performance and reduce the influence brought by delivering relief supplies.

VI. CONCLUSIONS

In rescue mission, parameters of quad rotor will change before and after delivering relief supplies. To ensure the control performance, a model reference adaptive control method is proposed. Firstly, the quad rotor model is established in Quanser 3-DOF hovering system. Then, a baseline controller is designed based on LQR. According to the closed-loop system consisted by LQR and linear model, an adaptive control law is carried out to reduce the impact of variable mass. Simulation results show that the MRAC method can make automatic adjustment to the change of parameters after delivering relief supplies.

ACKNOWLEDGMENTS

The authors thank the reviewers who gave a through and careful reading to the original manuscript. Their comments are greatly appreciated and have help to improve the quality of this paper. This work is supported by National Natural Science Foundation of China (No.61503255) and Natural Science Foundation of Liaoning Province (No.2015020063).

REFERENCES

[1] R. R. Murphy, B. A. Duncan, T. Collins, J. Kendrick, P. Lohman, T. Palmer, and F. Sanborn, “Use of a small unmanned aerial system for the SR-530 mudslide incident near Oso, Washington,” Journal of Field Robotics, vol. 33, pp. 476-488, 2016.

[2] J. Estevez, J. M. Lopez-Guede, and M. Grana, “Particle swarm optimization quadrotor control for cooperative aerial transportation of deformable linear objects,” Cybernetics and Systems, vol.47, pp. 4-16, 2016.

[3] J. P. Ortiz, L. I. Minchala, and M. J. Reinoso, “Nonlinear robust H-Infinity PID controller for the multivariable system quadrotor,” IEEE Latin America Transactions, vol.14, pp. 1176-1183, 2016.

[4] Y. M. Chen, Y. L. He, and M. F. Zhou. “Decentralized PID neural network control for a quadrotor helicopter subjected to wind disturbance,” Journal of Central South University, vol. 22, pp. 168-179, 2015.

[5] X. H. Lu, J. B. Li, and W. J. Liu. “A study of complementary filter algorithm for four-rotor helicopters attitude control system,” Sensors and Transducers, vol. 174, pp. 298-306, 2014.

[6] R. R. Benrezki, M. Tadjine, F. Yacef, and O. Kermia, “Passive fault tolerant control of quadrotor UAV using a nonlinear PID,” 2015 IEEE International Conference on Robotics and Biomimetics, Zhuhai, China, pp. 1285-1290, 2015.

[7] B. Mohd, A. Mohd, A. R. Husain, and K. A. Danapalasingam, “Backstepping controller with intelligent parameters selection for stabilization of quadrotor helicopter,” Journal of Engineering Science and Technology Review, vol. 7, pp. 66-74, 2014.

[8] A. Modirrousta, and M. Khodabandeh, “A novel nonlinear hybrid controller design for an uncertain quadrotor with disturbances,” Aerospace Science and Technology, vol. 45, pp. 294-308, 2015.

[9] Y. C. Choi, and H. S. Ahn, “Nonlinear control of quadrotor for point tracking: actual implementation and experimental tests,” IEEE/ASME Transactions on Mechatronics, vol. 20, pp. 1179-1192, 2015.

[10] F. Yacef, O. Bouhali, and M. Hamerlain, “Adaptive fuzzy backstepping control for trajectory tracking of unmanned aerial quadrotor,” 2014 International Conference on Unmanned Aircraft Systems, Orlando, FL, United states, pp. 920-927, 2014.

[11] J. Ghomman, G. Charland, and M. Saad, “Three-dimensional constrained tracking control via exact differentiation estimator of a quadrotor helicopter,” Asian Journal of Control, vol. 17, pp. 1093-1103, 2015.

[12] A. R. Merheb, H. Noura, and F. Bateman, “Design of passive fault-tolerant controllers of a quadrotor based on sliding mode theory,” International Journal of Applied Mathematics and Computer Science, vol. 25, pp. 561-576, 2015.

[13] K. D. Do, “Path-tracking control of stochastic quadrotor aircraft in three-dimensional space,” Journal of Dynamic Systems, Measurement and Control, Transactions of the ASME, vol. 137, pp. 1-11, 2015.

[14] B. Xian, C. Diao, B. Zhao, and Y. Zhang, “Nonlinear robust output feedback tracking control of a quadrotor UAV using quaternion representation,” Nonlinear Dynamics, vol. 79, pp. 2735-2752, 2015.

[15] H. Boudjedir, O. Bouhali, and N. Rizoug, “Adaptive neural network control based on neural observer for quadrotor unmanned aerial vehicle,” Advanced Robotics, vol. 28, pp. 1154-1164, 2014.

[16] Y. Yueneng, W. Jie, and Z. Wei, “Variable structure attitude control for an UAV with parameter Uncertainty and external disturbance,” 2011 International Conference on Advanced in Control Engineering and Information Science, Dali, Yunnan, China, pp. 408-415, 2011.

[17] J. Zhang, H. Xu, D. Zhang, and D. Liu, “Safety modeling and simulation of multi-factor coupling heavy-equipment airdrop,” Chinese Journal of Aeronautics, vol. 27, pp. 1062-1069, 2014.

[18] J. O. Pedro, A. Panday, and L. Dala, “A nonlinear dynamic inversion-based neurocontroller for unmanned combat aerial vehicles during aerial refueling,” International Journal of Applied Mathematics and Computer Science, vol. 23, pp. 75-90, 2013.

[19] Quanser, 3-DOF Control Manual, 2008, http://www.quanser.com/Products/3dof_hover

[20] C. Pedro, L. Rogelio, and E. D. Alejandro, “Modeling and Control of Mini-Flying Machines,” Springer: London, pp. 142-147, 2005.

[21] F. Chen, F. Lu, B. Jiang, and G. Tao, “Adaptive compensation control of the quadrotor helicopter using quantum information technology and disturbance observer,” Journal of the Franklin Institute, vol. 351, pp. 442-455, 2014.